Pierre Colinet
Alexander Nepomnyashchy
Editors

International Centre
for Mechanical Sciences

Pattern Formation at Interfaces

CISM Courses and Lectures, vol. 513

SpringerWienNewYork

SpringerWienNewYork

CISM COURSES AND LECTURES

The series presents lecture notes, monographs, edited works and proceedings in the field of Mechanics, Engineering, Computer Science and Applied Mathematics.
Purpose of the series is to make known in the international scientific and technical community results obtained in some of the activities organized by CISM, the International Centre for Mechanical Sciences.

INTERNATIONAL CENTRE FOR MECHANICAL SCIENCES

COURSES AND LECTURES - No. 513

PATTERN FORMATION AT INTERFACES

EDITED BY

PIERRE COLINET
UNIVERSITE LIBRE DE BRUXELLES, BRUSSELS, BELGIUM

ALEXANDER NEPOMNYASHCHY
TECHNION-ISR. INST. OF TECHNOLOGY, HAIFA, ISRAEL

SpringerWienNewYork

This volume contains 113 illustrations

Printed in Italy
SPIN 12821907

All contributions have been typeset by the authors.

ISBN 978-3-7091-0124-7 SpringerWienNewYork

PREFACE

Interfacial pattern formation occurs in several natural, technological and medical contexts such as, e.g., water films and droplets flowing along inclined surfaces, drying of paint films or coatings, electro-deposition, semiconductor processing, micro-fluidics, mucus flow in the lungs, dry eye syndrome... Modeling these processes requires an understanding of their physics and the knowledge of length and time scales that characterize them. Interfaces play a dominant role at small scales, and their correct modeling is therefore also crucial in the rapidly expanding field of nano-technology (e.g. self-organized nano-particle deposition patterns, quantum dots, ...).

The need to compare various descriptions of the physics of multi-scale interfacial phenomena and the desire to help newcomers in the field in mastering their modeling and identifying modern scientific and technological challenges, inspired the organization of the CISM Advanced School "Pattern Formation at Interfaces with Applications to Materials Science, Biomedical and Physico-Chemical Processes" which took place in Udine, Italy, October 16-20, 2006. Six lecturers from Belgium, Germany, Israel and the USA gave series of lectures to an audience of graduate students, postdocs and young researchers. The lectures have covered most modern methods allowing to treat interfacial instabilities, such as multi-scale asymptotic expansions, linear stability, weakly nonlinear methods and bifurcation theory. Analytical and fully numerical techniques have been discussed, and experimental results have been presented either to confirm theory, or to illustrate directions for further research.

The present book consists of six chapters inspired from the lectures given during the CISM Advanced School. All contributions are presented within the framework of continuous theories and transport phenomena, i.e. mass, momentum and heat transfer. Yet, the investigation of phenomena taking place at interfaces and fronts of phase transition needs the combination of two different kinds of models. In the first approach, the interfaces or the fronts are considered as objects of zero thickness, while the second approach recognizes the internal "diffuse" structure of the transition zone.

The dynamics of interfaces and fronts are characterized by numerous kinds of instabilities leading to nonlinear patterns and waves.

Several challenging physical problems such as phase transition instabilities, front velocity selection and transitions to chaotic spatio-temporal regimes, are discussed with a view of identifying the relevant physico-chemical processes and taking into account multi-scale couplings at theoretical and numerical level, in a rigorous manner. Generic aspects of nonlinear phenomena are also emphasized and to complete the picture, experimental evidence of pattern formation at interfaces is provided to illustrate and validate modeling approaches.

The book is intended to graduate students, researchers and lecturers in physics and engineering, interested in mastering the modern methods of nonlinear stability theory applied to the problems of continuous media mechanics in the presence of interfaces, with applications to materials science, chemical engineering, heat transfer technologies, as well as in combustion and other reaction-diffusion systems. The readers are expected to have followed a first level course in fluid mechanics or transport phenomena and some background in linear algebra, ordinary and partial differential equations. Other goals of this volume are to allow the reader to identify key problems of scientific value, the methods to resolve modeling issues, and to see the similarity between a variety of seemingly different physical problems. Reading the book and some of the references cited therein should allow the reader to quickly move into an area of physics and engineering that is rich in phenomena and replete in applications.

The idea of carrying out this CISM Advanced School on pattern formation at interfaces belongs to Professor Manuel G. Velarde, while he was actually Rector of CISM. Its realization would not have been possible without his encouragement and help. This book is dedicated to him, and to his essential contributions to the field.

Tragically, one of the authors of the present book, Professor Alexander (Sasha) Golovin, passed away in September 2008, while this book was in preparation. This is a great loss for his friends and for the whole "nonlinear science community". Many of us benefited much from scientific discussions and collaboration with this exceptional person who never stopped smiling. According to the students and colleagues who followed the School, his lectures were an example of combined rigor, great enthusiasm for Science, and pedagogy. We will never forget him.

Alexander Nepomnyashchy and Pierre Colinet

CONTENTS

Interfacial patterns and waves in liquid layers and thin films

Pierre Colinet*

Laboratory TIPs (Transfers, Interfaces and Processes) – Fluid Physics Unit,
Université Libre de Bruxelles, C.P. 165/67, 50 av. F.D. Roosevelt,
B-1050 Bruxelles, Belgium

Abstract This chapter describes the phenomenology and modeling of Bénard-like patterns and waves in liquid layers, including the case of thin films for which surface tension effects are dominant. Attention is also paid to the (generalized) one-sided description of instabilities in the presence of evaporation, with or without an inert component in the gas phase. Then, the focus is on simplified models of patterned structures, and on the role of symmetry properties of the physical system considered.

Contents

*Research Associate (Fonds de la Recherche Scientique - FNRS)

1 Introduction

Natural convective flows in fluid layers submitted to temperature and/or concentration gradients can be induced either by density gradients and associated buoyancy, or by surface tension gradients. As most of this text is devoted to the latter mechanism, and for readers unfamiliar with the topic, it is worth describing first the origin of the so-called Marangoni effect in greater details. Interfacial (or surface) tension at the boundary between two different fluid phases originates from the long-range attractive forces between molecules, i.e. the forces which are responsible for the cohesion of a condensed phase (Israelachvili, 1992). In the case of a liquid-gas interface for instance, molecules in the liquid bulk are attracted by neighboring molecules in an isotropic way, while those located in the interfacial region are globally attracted towards the liquid phase, as they practically do not feel the presence of much more distant gas molecules. Consequently, surface molecules are in an energetically unfavorable situation, which the liquid will tend to avoid as far as possible, by adopting a spherical shape (in the absence of other forces such as gravity or adhesion forces with a solid). Surface tension can be defined as the energy necessary to create a unit surface area, indeed positive since it requires bringing molecules from the bulk to the surface.

Surface tension is generally decreasing with temperature, for most liquids like water or oils. Therefore, when a free surface[1] is non-isothermal, the resulting inbalance of intermolecular forces leads to a macroscopic tangential stress, which occurs from the warmer portions of the surface to the colder parts, hence generating a flow. This thermocapillary (or Marangoni) flow may be seen as a way for the system to reduce regions of high surface tension by enlarging regions of low surface tension. Note that in case gradients of surface tension result from concentration differences along the surface of a liquid mixture, one rather speaks about a "solutal" Marangoni (or solutocapillary) effect.

Marangoni flows are commonly observed in everyday life, e.g. via the motion of dusts in the wax of a candle (see Fig. 1, left), the proximity of the flame being at a much higher temperature than the periphery of the candle. Another famous example is the phenomenon of "tears of wine" (see Fig. 1, right) whose mechanism is however far more complicated, involving preferential evaporation of the alcohol, wetting properties with glass, thermal and solutal Marangoni effects, and gravitational instability of fluid rising along glass walls. A tentative explanation of this phenomenon was

[1] We will generally use the term "free" surface for an interface between a liquid and a gas, or a liquid and its vapor.

given as early as in 1855 by James Thomson (Thomson, 1855), even though the Marangoni effect was given its name following the later work of Carlo Marangoni in the 1870's.

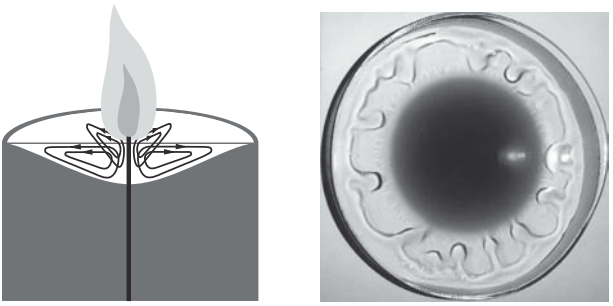

Figure 1. Left : thermocapillary flow in candle wax. Right : tears of wine in a glass viewed from above (Courtesy of John Bush and Anette Hosoi, MIT).

In these lectures, we will mostly be concerned with the phenomenology and modeling of thermal Marangoni flows generated in a liquid layer heated from below (see Fig. 2) or from above. In the former case, hexagonal structures were first observed by Henri Bénard (Bénard, 1901) at the beginning of the century (hence the name of Marangoni-Bénard flows), even though their correct interpretation in terms of the Marangoni effect was given much later (Block, 1956).

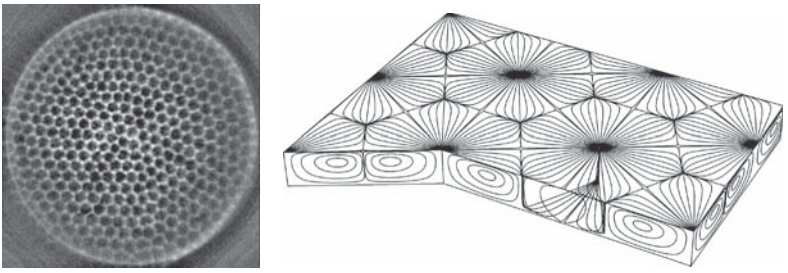

Figure 2. Left : hexagonal pattern observed by shadowgraphy, perpendicularly to the free surface of a liquid layer heated from below (Eckert et al., 1998), in a circular dish (Courtesy of Kerstin Eckert, Dresden University). Right : Theoretically calculated three-dimensional particle paths within steady hexagonal convection cells.

Generally speaking, several levels of modeling are possible : starting from the smallest time and length scales, molecular dynamics simulations can be undertaken, which certainly provide the most accurate description of interface structure and microscopic kinetics, though the computational cost of these techniques remains extremely high, especially for polyatomic molecules and large system sizes. At an intermediate (mesoscopic) level, methods based on the so-called diffuse-interface or phase-field theory have proven quite flexible and adequate to numerically simulate problems involving complex interface shapes and dynamical events such as rupture and coalescence. At the same level, lattice Boltzmann methods, proceeding on the basis of discrete models of the celebrated Boltzmann equation and its variants, also describe interfaces as non-zero thickness objects across which fluid quantities (density, concentration, ...) undergo sharp variations. Finally, at a macroscopic level, interfaces are modelled as zero-thickness surfaces of discontinuity along which adequate interfacial (jump) boundary conditions must be expressed. These lectures will exclusively be concerned with the latter approach, not only because significant progresses have been accomplished along these lines in the last decades (e.g., in connection with Nonlinear Physics), but also because it is now commonly admitted that macroscopic models may indeed be used down to very small scales, even in the submicrometer range.

Importantly, there exists a formal analogy between the problems of heat transfer involving thermocapillarity, and mass transfer associated with concentration gradients generating solutocapillary flows. Actually, the mathematical descriptions of such phenomena are quite similar, provided some complications specific with mass transfer through an interface are ignored, such as solute accumulation at the interface, adsorption kinetics, ... Consequently, at least in the simplest descriptions, it will be formally equivalent to say that a pure liquid layer is heated from below, or that a two-component isothermal liquid layer undergoes desorption through its upper free surface of the component which lowers the surface tension (hereafter called a surfactant). In the second situation considered in these lectures, a liquid layer is heated from the top (or undergoes absorption of a soluble surfactant). In these cases, one typically observes a self-organization of the system in the form of propagating wave trains, e.g. azimuthally in an annular container as in Fig. 3(left). Occasionally, simultaneous propagation of waves in both azimuthal directions may also be observed, such as in Fig. 3(right). Such wave trains have strong analogies with solitary waves, though their weak dissipation on a large time scale can here be balanced by energy input from an underlying instability. These interesting aspects have been studied in details by Velarde and co-workers (see e.g. Christov and Velarde, 1995;

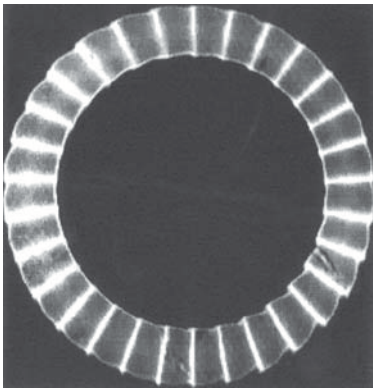

Figure 3. Left : azimuthally-propagating wave trains visualized by a shadowgraph technique during absorption of pentane vapor into toluene (Courtesy of Andreas Wierschem). Right : counter-propagating wave trains observed in a heat transfer experiment with heating from the top (after Weh and Linde, 1997).

Rednikov and Velarde, 2000).

Both cases of heating from above or below (absorbing or desorbing a surfactant) therefore lead to a spontaneous breaking of the natural symmetries of the Bénard layer, either in the form or waves, or of steady convection patterns. Indeed, in case a flux (either of heat or of matter) occurs perpendicularly to an interface, surface tension is expected to be uniform, i.e. no flow is expected *a priori*. In mathematical terms, the system is invariant with respect to translations along its interface (in the idealized case of a laterally infinite layer), and enjoys isotropy as well, i.e. any rotation with respect to an axis orthogonal to the layer leaves the latter unaffected. Symmetry-breaking associated with the emergence of ordered structures in non-equilibrium systems is typical of instability phenomena (see other examples in the same volume), among which surface-tension-driven (and buoyancy-driven) instabilities discussed in these lectures.

2 Phenomenology of Bénard instabilities

2.1 Physical mechanisms of patterns and waves

Let us first consider the so-called Rayleigh–Bénard instability (Fig. 4, left), associated with buoyancy-driven (rather than surface-tension-driven) convection. A layer of pure liquid (which will be considered as incompress-

ible and Newtonian) is confined between two horizontal plates maintained at controllable temperatures.

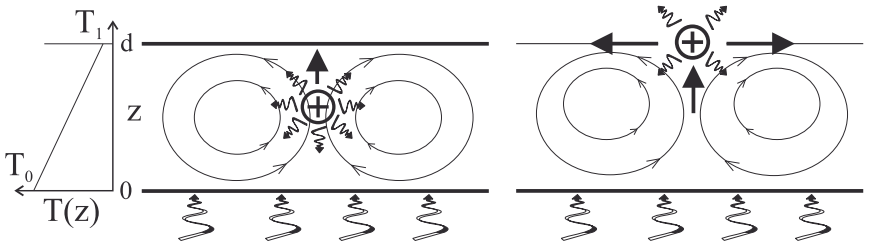

Figure 4. Sketches illustrating the mechanisms at the origin of the Rayleigh–Bénard (left) and the Marangoni–Bénard (right) instabilities. In both cases, the temperature of the bottom plate is T_0 while that of the upper surface (either solid or open to air) is $T_1 < T_0$ (the layer is heated from below).

Assume for the moment that the dissipative effects of molecular transport of heat and momentum are negligible (i.e. associated with very long time scales, see §2.3). Then, when a localized fluctuation of temperature (say, a hot spot) arises in a certain volume element, an upward force on this fluid particle is induced by buoyancy, as its density is decreased compared with its environment (differential buoyancy force). As molecular diffusion is assumed to be negligible, the fluid particle will set into motion in the upward direction, without friction, and will remain at the same temperature during this motion. The buoyancy force it will experience will then increase, because the particle moves towards colder regions, such that the velocity is increased, ... This is the origin of the amplification (instability) phenomenon.

The Marangoni-Bénard mechanism may be explained similarly (Fig. 4, right) : if a fluctuation of temperature (say, a hot spot) occurs at the free surface (or interface), a local surface tension gradient is created, directed radially away from the fluctuation. The associated tangential stresses then induce radially divergent surface fluid motion (the interface may be seen as an elastic membrane which relaxes at the point where the disturbance is created). Now, continuity of the fluid requires a vertical ascending flow to take place below the disturbance. If the layer of fluid is heated from below, this uprising fluid, being hotter, will make the free surface temperature increase at the initial location of the disturbance. Consequently, the surface tension at that point decreases, thus increasing the tangential stresses.

Clearly, thermal diffusivity will act against these instability processes,

by favoring thermalization of fluid particles with their environment, i.e. damping of fluctuations. Viscosity will also generate stresses, preventing macroscopic motions to develop within the fluid. As a result, the temperature difference $\Delta T = T_0 - T_1$ has to exceed a threshold value for Bénard instabilities to develop, in order for the destabilizing mechanisms to overcome the dissipative effects. This will be quantified in terms of time scales and dimensionless numbers in §2.3.

Note that contrary to the Marangoni-Bénard instability leading to hexagons (see Fig. 2) when the instability threshold is exceeded, the Rayleigh-Bénard instability typically yields roll patterns, the study of which has motivated important progresses in the theory of pattern formation (see for instance Cross and Hohenberg, 1993). Note that both rolls and hexagons are very seldom perfectly regular, and various kinds of defects have indeed been observed, and studied extensively for their interesting universal properties. For instance, hexagonal patterns very often display isolated pentagon-heptagon defects, which can act as mediators in the transition from hexagonal to square patterns observed at increasing temperature difference ΔT, via a process of nucleation of lines of pentagons (Eckert and Thess, 1999).

Considering now the opposite case of a liquid layer heated from above, first in the buoyancy-driven case, it is quite natural to expect an oscillatory behavior of fluctuations, again in the case where the effect of dissipation is not too strong. Indeed, during its upward motion, a fluid particle initially warmer than its environment will now move towards *warmer* regions. This means that the upward buoyancy force it experiences will first decrease, then eventually change sign when the particle overshoots its neutrally buoyant position, due to inertia. The particle is then accelerated downwards, towards colder regions, and may oscillate around its neutrally buoyant position several times before dissipation eventually damps out any fluid motion. This oscillatory mechanism is known in the literature as (Brunt–Väisälä) internal waves, observed in situations of stable density stratification (e.g. in the atmosphere or the ocean, see Turner, 1973).

Similarly, surface waves due to thermocapillarity in a layer heated from above are also expected, and may be explained considering once again a hot spot at the free surface. As usual the Marangoni effect drives a surface flow away from the spot, which now brings *colder* liquid from the bulk. Because of fluid inertia, the initially hot spot eventually becomes colder than its neighborhood (overshoot), thus reversing the flow and leading to oscillations. These waves involve motions essentially parallel to the free surface, and may be called longitudinal waves for this reason.

Note that both internal and surface waves are usually damped, though

it has been shown recently (Rednikov et al., 2000) that their interaction near resonance may lead to amplification and mode-mixing (see section 3.4). Actually, internal waves excited by the Marangoni effect are indeed thought (Wierschem et al., 2000) to be responsible for the propagating wave trains shown in Fig. 3(left), i.e. in a situation where pentane is absorbed in toluene. Given that pentane is lighter than toluene, absorption indeed generates a stable density stratification prone to triggering of internal waves by external disturbances, just as in the thermal case discussed above. As pentane also lowers the surface tension of the mixture, longitudinal surface waves may also occur and resonantly interact with (transverse) internal waves.

Finally, the well-known capillary-gravity waves are yet another oscillatory mode, which occurs whenever a free surface is perturbed by an external force. Ripples propagating along a free surface involve an essential deformation orthogonal to the latter, and are transverse waves in this respect. Interestingly, such capillary-gravity waves may also be excited in layers heated from the top, via resonant interaction and mixing with the surface longitudinal waves just discussed (Rednikov et al., 2001). A review of experimental findings on waves generated by heat or mass transfer through an interface, their interpretation in terms of internal, surface and capillary-gravity waves, as well as their links with solitary waves, are given in the book of Nepomnyashchy et al., 2002.

2.2 Application-oriented aspects

When a layer of fluid is heated from below, the state of pure conduction prevailing at small ΔT is first replaced by a cellular convective structure at a certain ΔT_c, as explained in the previous section. Convective heat transport now adding to the effect of heat conduction, the global heat transfer through the layer is enhanced, which may be seen as an increase of the apparent thermal conductance (or heat transfer coefficient) of the liquid layer (defined, e.g., by $\Phi/\Delta T$ where Φ is the mean heat flux crossing the layer). Subsequent transitions, e.g. to time-dependent regimes, generally result in further increases of the heat transfer coefficient. This has been extensively studied for the case of Rayleigh-Bénard convection, even in the regimes of so-called weak and strong thermal turbulence setting in at very high $\Delta T/\Delta T_c$ (see for instance Guyon et al., 1991).

In surface-tension-driven situations, much less is known, even though interfacial turbulence has been observed as early as in the 50's, in the context of Chemical Engineering. In many situations involving interfacial heat and mass transfer (for instance in techniques such as liquid/liquid extraction,

liquid/gas absorption or desorption, distillation, ...), order of magnitude changes of transfer rates from one phase to another have been measured and correlated with empirical relationships. An extensive review of such phenomena and a rather complete bibliography are provided in the thesis of T. Molenkamp (Molenkamp, 1998). Note also that in chemical reactors, mass transfer through interfaces is often accompanied by chemical reactions, and interesting couplings with surface-tension-driven convection can occur (Eckert and Grahn, 1999; Eckert et al., 2004).

Marangoni–Bénard convection is also important in processes involving evaporation, such as in the drying of paint films, in the coating industry, and for heat transfer devices. In Fig. 5, a thin layer of ethyl alcohol is evaporated under an inert gas (nitrogen) flow. Even though no external heating is imposed in this experiment, cellular convection develops as soon as the flow is imposed, due to the cooling of the free surface induced by evaporation (consumption of latent heat). The fact that these convective patterns are sustained by evaporation is further confirmed by their sudden disappearance when vapor removal by the gas flow is interrupted (images 8 and 9). In turn, convective transport of heat reduces the overall thermal resistance of the liquid layer, therefore contributing to an increase of the evaporation rate.

In addition to the increase of the interfacial exchange coefficients (i.e. per unit surface), Marangoni flows often induce significant interfacial deformation, leading to important variations of the total surface of exchange itself. In the case of thin liquid films, specific instabilities (see §2.4) may occur, leading in some cases to dry regions. While such dry spots are generally unfavorable (for instance, in thin-film evaporators, they lead to possible overheating and destruction of the substrate), they also have a positive effect since the heat transfer resistance scales proportionally to the local film thickness, as a first approximation. As a consequence, the local heat flux can become locally very high in the transition region between the film and the dry spot (i.e. at the contact line), as was quantified by P. Stephan in the context of heat-transfer devices such as heat pipes and boilers (Stephan and Busse, 1992).

Generally speaking, Marangoni effects and associated instabilities are expected to be dominant at small length scales, where gravity and buoyancy are ineffective (as will be seen from dimensionless groups in the next section). There is therefore a renewed interest in recent years, especially in connection with the rapidly developing fields of microfluidics and even nanotechnologies. At such scales, self-organization phenomena such as the surface-tension-driven Bénard instability could for instance be used as a way to design special types of solid surfaces, by deposition of nanocrystals

in the forms of polygonal arrays and rings (see e.g. Maillard et al., 2000).

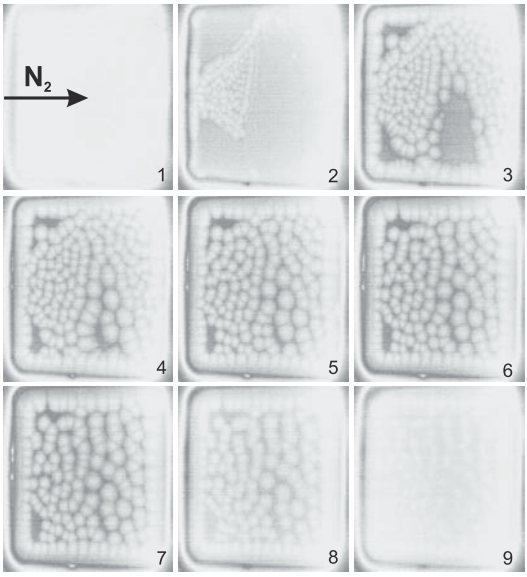

Figure 5. Sequence of infrared camera images of the free surface of a thin liquid layer of ethyl alcohol, forced to evaporate under a flux of nitrogen (indicated by the arrow) at room temperature and atmospheric pressure.

2.3 Dimensionless numbers and time scales

Several time scales can be defined from physical properties of the fluid and geometrical characteristics such as its depth d. We first have the thermal time scale

$$\tau_{\rm th} = \frac{d^2}{\kappa} \tag{1}$$

i.e. the typical time scale it takes for temperature fluctuations to be damped over a distance d (κ is the thermal diffusivity[2]). Similarly, velocity (or

[2]In this section, we will generally refer to a pure fluid submitted to a temperature difference ΔT. However, for an isothermal binary fluid, similar time scales and dimensionless numbers may be defined, replacing ΔT by ΔN (a typical mass fraction difference between bottom and top), κ by D (the isothermal diffusion coefficient), and defining $\gamma = -(\partial\sigma/\partial N)$ and $\alpha = -(\partial\rho/\partial N)/\rho$, where σ and ρ are the surface tension and the volumic mass, respectively.

vorticity) fluctuations decay on a viscous time scale

$$\tau_{\rm visc} = \frac{d^2}{\nu} \tag{2}$$

where ν is the kinematic viscosity.

Now, it is possible to construct two other time scales which do not depend on any molecular diffusivity mechanism. The first one is the "buoyancy time scale"

$$\tau_{\rm buoy} = \sqrt{\frac{d}{\alpha g \Delta T}} \tag{3}$$

which is roughly the time it takes for a fluid particle at the bottom of the layer to be accelerated by buoyancy up to its upper surface (see Fig. 4), i.e. the typical time scale of the instability leading to convective patterns. In Eq. (3), α is the thermal expansion coefficient, g is the gravity acceleration, and $\Delta T = T_0 - T_1$ is the temperature drop across the layer.

Similarly, a typical time scale of the thermocapillary (or Marangoni) instability can be defined as

$$\tau_{\rm ma} = \sqrt{\frac{\rho d^3}{\gamma \Delta T}} \tag{4}$$

where ρ is the liquid volumic mass, and $\gamma = -\partial\sigma/\partial T$ is the coefficient of variation of surface tension with temperature (positive for usual liquids).

Note that when the layer is heated from the top, $|\tau_{\rm buoy}|^{-1}$ and $|\tau_{\rm ma}|^{-1}$ provide order of magnitude estimates of the frequencies of internal and surface waves (see §2.1), respectively.

Comparing the different time scales given by Eqs (1–4), it may be expected that instability will develop if the time for a fluid particle to travel over a distance of order d is shorter than the times necessary for the particle either to be slowed down by viscosity, or thermally equilibrated with its environment. Thus, buoyancy-driven instability would occur typically if

$$Ra = \frac{g\alpha\Delta T d^3}{\nu\kappa} = \frac{\tau_{\rm visc}\tau_{\rm th}}{\tau_{\rm buoy}^2} \gg 1 \tag{5}$$

while surface-tension-driven instability will occur when

$$Ma = \frac{\gamma \Delta T d}{\rho\nu\kappa} = \frac{\tau_{\rm visc}\tau_{\rm th}}{\tau_{\rm ma}^2} \gg 1 \tag{6}$$

These equations define both the Rayleigh number Ra and the Marangoni number Ma, which are the usual measures for the relative importance of

destabilizing and stabilizing effects. Typically, the critical value of the Rayleigh number above which instability sets in is of order 10^3, while the critical Marangoni number is of order 10^2. Their actual values depend on the nature of upper and lower plates (e.g. rigid and heat-conducting, or free and poorly-conducting, ...), and must be determined by linear stability analysis (see §3.4).

Note that other usual dimensionless parameters are the Prandtl number $Pr = \nu/\kappa = \tau_{\rm th}/\tau_{\rm visc}$ and the Galileo number $Ga = gd^3/\nu\kappa = \tau_{\rm th}\tau_{\rm visc}/\tau_{\rm grav}^2$ where $\tau_{\rm grav} = (d/g)^{1/2}$, i.e. the typical time scale for a body to be accelerated over a distance d under the action of gravity.

Finally, in case the liquid layer presents an upper free surface, it is common to describe heat transfer through the latter using a constant heat transfer coefficient h (or a constant Biot number $Bi = hd/\lambda$ in dimensionless form, where λ is the liquid thermal conductivity). Even though this is a crude approximation since the heat transfer coefficient generally depends on convective motions in the gas phase, and therefore on the temperature of the interface itself, it does provide the correct tendency for the influence of heat transfer at the upper surface (namely an increase of the critical Marangoni number with increasing Biot number). A more rigorous definition of a "generalized Biot number" will be presented in §3.

2.4 Other instability mechanisms in very thin liquid films

Yet another instability mode can occur, specifically for thin liquid films of viscous liquids. This is illustrated in Fig. 6 : consider that an initially flat heated liquid film (top figure) is perturbed, resulting in a non-uniform liquid depth (middle figure). At the thinner parts of the film, the free surface is warmer (since it is closer to the heated plate) than at thicker regions. A surface tension gradient therefore arises, and generates a flow dragging fluid away from the depression, hence depleting the thinner parts even more. This may result in the formation of dry spots (bottom figure), even though the correct description of the film evolution near rupture should involve intermolecular forces between the fluid and the substrate, typically when the local thickness decreases below 100 nm (Israelachvili, 1992; Oron et al., 1997).

Note that the horizontal length scale of convective motions (and of surface deformations) generated by this mechanism is generally much larger than the fluid depth, hence the name long-wave deformational mode for this instability mechanism. In contrast, polygonal convection cells typical of Marangoni-Bénard convection turn out to scale proportionally to the depth of the liquid layer (see Fig. 2) in case the rigid bottom plate is a

good thermal conductor (such as a metal). In case the bottom plate has a low heat transfer coefficient, just as the upper free surface, the Marangoni-Bénard convection cells become large-scale as well, which offers a way to describe them in terms of long-wave asymptotic theories.

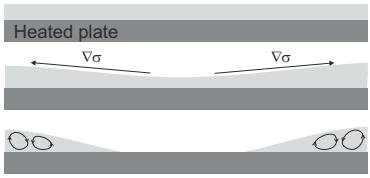

Figure 6. Long-wave deformational instability of heated thin liquid film.

The long-wave deformational mode occurs typically for $Ma > Ma_0 \sim Ga$, for a purely insulating upper free surface (a good approximation for liquids in contact with a gas phase). As introduced in the previous section, the Galileo number $Ga = gd^3/\nu\kappa$ measures the stabilizing influence of gravity on surface deformations, and is usually extremely large ($\sim 10^8$!) for usual fluids with depths in the centimeter range. In these cases, cellular convection mechanisms will always occur first, since their critical Marangoni number is typically 10^2 (actually, for depths larger than about 1 cm, buoyancy-driven convection dominates, while surface-tension-driven convection is most effective at depths below some millimeters).

For very thin layers of highly viscous liquids however, long-wave deformational modes may become active, and a fortiori the primary instability mode when the long-wave threshold $Ma_0 \sim Ga$ becomes lower than the usual threshold $Ma_c \sim 10^2$ for cellular Marangoni-Bénard convection. While for water this corresponds to unusually thin liquid films ($d \sim 100$ μm or less), this becomes experimentally accessible with highly viscous liquids such as silicone oils [e.g. for a 200 cSt oil, $Ma_0 \sim Ga \sim 10^2$ for $d \simeq 0.6$ mm]. Recent experimental results of VanHook et al. (VanHook et al., 1997) have indicated that the cross-over between the two modes may indeed be observed, possibly resulting in coexistence of large-scale dry spots with depth-scaled convection cells such as sketched in Fig. 6 (bottom). VanHook et al. have further observed and explained that the long-wave deformational mode indeed generally leads to film rupture (see also Oron et al., 1997), but more complex situations may occur (surface elevations or "high spots", cascades of structures, ...). Note that situations involving essential surface deformation will not be considered further in these notes, as they will be described in details in the lectures of M. Bestehorn and L. Pismen, including the de-

scription of rupture of ultrathin films due to molecular interactions with the substrate, droplets, ...

3 Basic equations and boundary conditions

Even though the description of Bénard instabilities in layers with a free surface generally involves fluid motions and temperature fluctuations in both liquid and gas phases (two-layer system), it is often possible to make some simplifying assumptions (given hereafter) in order to describe them in terms of liquid quantities alone (one-sided model), with suitable boundary conditions. Using the thermal time scale $\tau_{\rm th} = d^2/\kappa$, the length scale d, the pressure scale $\mu\kappa/d^2$, and a yet undefined temperature range θ, the basic dimensionless equations generally used to describe thermally-driven Bénard instabilities of a liquid layer are

$$\vec{\nabla} \cdot \vec{V} = 0 \tag{7}$$

$$\Delta\vec{V} - \vec{\nabla}p - Ga\vec{1}_z[1 - \alpha\theta(T - \tilde{T}_{\rm r})] = Pr^{-1}\left(\frac{\partial\vec{V}}{\partial t} + (\vec{V}\cdot\vec{\nabla})\vec{V}\right) \tag{8}$$

$$\Delta T = \frac{\partial T}{\partial t} + (\vec{V}\cdot\vec{\nabla})T \tag{9}$$

where $\vec{V} = (U, V, W)$, T, and p are respectively the dimensionless fields of velocity, temperature and pressure, $\vec{1}_z$ is the unit vector directed vertically upwards, $\tilde{T}_{\rm r} = (T_0 + T_1)/2\theta$ is the dimensionless reference (mean) temperature at which the physical properties are evaluated (note that their possible variation is neglected, in the temperature range θ considered), and other dimensionless quantities have been defined earlier. Equations (7-9) respectively express the conservation of mass (for incompressible liquids), of momentum (in the presence of a buoyancy force), and of energy (neglecting viscous heating).

Importantly, this form of the equations makes use of the Boussinesq approximation, i.e. $|\alpha\theta| \ll 1$. This means that the variations of density may be neglected everywhere, unless when multiplied by large quantities such as the Galileo number Ga, as it indeed occurs for the body force term of the Navier-Stokes equations (8). Actually, the Rayleigh number (defined using the temperature range θ) is the product $Ra = \alpha\theta Ga$, i.e. the product of a small and a large number, and can therefore be sufficient to trigger instability of the Bénard layer.

Boundary conditions on the bottom plate $z = 0$ are usually taken as the no-slip and constant temperature conditions

$$\vec{V} = T - T_{bot} = 0 \quad \text{at } z = 0 \tag{10}$$

where $T_{bot} = \theta^{-1} T_0$, while those at the upper free surface should in principle be written at a unknown position, which should be found as a solution of the full problem. However, we will not deal with such deformable free surfaces here (the reader is referred to the book of Colinet et al., 2001, for general interfacial conditions) and assume the free surface to be located at $z = 1$, i.e. disregarding the case of very thin liquid films (the effect of gravity, quantified by the Galileo number, is sufficiently strong to prevent free surface deformations).

In addition, as mentioned above, a coupling of liquid and gas phases is expected at $z = 1$. We now underline the main hypotheses necessary to reach a one-sided description, i.e. to write the correct number of free surface boundary conditions, though in terms of liquid quantities alone.

First, the liquid velocity orthogonal to the interface is zero, since it is assumed motionless. Hence,

$$W = 0 \quad \text{at } z = 1 \tag{11}$$

Second, in view of the fact that the dynamic viscosity of the gas is generally much lower than that of the liquid, we may neglect gas viscous stresses in the tangential momentum balance at $z = 1$. Taking into account surface tension gradients and in dimensionless form, this reads

$$\partial_z U + Ma\, \partial_x T = \partial_z V + Ma\, \partial_y T = 0 \quad \text{at } z = 1 \tag{12}$$

where $Ma = \gamma \theta d / \rho \nu \kappa$ is the Marangoni number. Note that an equivalent form is obtained by differentiating the first of these boundary conditions with respect to x, the second with respect to y, adding the results and using the incompressibility condition (7). This yields

$$\partial_z^2 W = Ma\, \Delta_{\mathrm{h}} T \quad \text{at } z = 1 \tag{13}$$

where $\Delta_{\mathrm{h}} = \partial^2/\partial x^2 + \partial^2/\partial y^2$ is the horizontal Laplacian operator.

A straightforward way to close the problem would be to neglect the thermal conductivity of the gas, and therefore to assume $\partial_z T = 0$ at the free surface (zero heat transfer coefficient). Under some assumptions mentionned in section 3.2, evaporation can also be included in the energy conservation at the interface, which yields

$$\partial_z T = -EJ \quad \text{at } z = 1 \tag{14}$$

where $E = L/c_p\theta$ is an evaporation number, comparing the latent heat of evaporation L to $c_p\theta$, i.e. the heat needed to warm up the liquid over the

selected temperature range θ. Note that Eq. (14) introduces the evaporation rate J (here scaled by $\rho\kappa/d$), which is often written as

$$J = \beta\sqrt{\frac{M}{2\pi R\, T_{sat}}}\, p'_{eq}(T_{sat})\frac{\theta d}{\rho\kappa}(T - \theta^{-1}T_{sat}) \tag{15}$$

i.e. one of the possible forms of the Hertz-Knudsen kinetic law (see also Burelbach et al., 1988), in which β is the accomodation coefficient, M is the liquid molecular mass, R is the universal gas constant, $p_{eq}(T)$ is the equilibrium pressure at temperature T (e.g. the Clausius-Clapeyron coexistence curve), and T_{sat} is the (dimensional) saturation pressure at the local vapor pressure p_v, i.e.

$$p_{eq}(T_{sat}) = p_v \tag{16}$$

Hence, for a pure vapor phase where the vapor pressure p_v may be assumed constant, T_{sat} is a constant and Eqs (14) and (15) combine to give a mixed thermal condition

$$\partial_z T + Bi_{ev,p}(T - \theta^{-1}T_{sat}) = 0 \tag{17}$$

where the effective heat transfer coefficient (i.e. the Biot number, in dimensionless form) reads

$$Bi_{ev,p} = \beta\sqrt{\frac{M}{2\pi R T_{sat}}}\, p'_{eq}(T_{sat})\frac{Ld}{\lambda} \tag{18}$$

and the index p stands for "pure vapor phase". Note that the values calculated for $Bi_{ev,p}$ are generally very high apart for very thin liquid films or very small accomodation coefficient[3], such that the interfacial temperature remains everywhere very close to T_{sat} (local thermodynamic equilibrium between the vapor and the liquid), and the Marangoni effect is very weak.

Hence, the problem is now closed, either for the case where the liquid is non-volatile and the vapor phase has very small thermal conductivity ($Bi_{ev,p}$ has to be set to zero in Eq. (17)), or when the liquid can evaporate into its own vapor (in which case $Bi_{ev,p}$ is a very large quantity). However, there are cases where one or both of these assuptions fail, and a more general approach is needed.

[3] As also discussed by Colinet et al., 2001, the cross-over between the reaction-limited regime $Bi_{ev,p} \ll 1$ and the heat transfer-limited regime $Bi_{ev,p} \gg 1$ occurs for a depth $d =$O(100 nm), for water near the normal boiling point and an accomodation coefficient $\beta = 1$. This depth increases when β decreases, however.

3.1 Non-negligible gas thermal conductivity

As the assumption of vanishing gas thermal conductivity may not be justified in all cases (e.g. helium is equally conducting as a silicone oil), it seems preferable to generalize the rough approach of the previous section, though first in the non-volatile case.

In general, the thermal diffusivity κ_g of a gas is about one hundred times larger than that of a liquid. Therefore, the time scale of thermal fluctuations in the gas, i.e. d_g^2/κ_g (where d_g is the gas depth), is much smaller than the liquid thermal time scale $\tau_{th} = d^2/\kappa$. In addition, we may also expect the energy transport due to gas flows to be negligible compared with thermal diffusion (small Péclet number assumption[4]), and the energy equation in the gas may be written in the quasi-steady approximation

$$\Delta T_g = 0 \tag{19}$$

which may in principle be solved using boundary conditions $T_g = T(x, y, z = 1, t)$ at $z = 1$ and $T_g = T_{up}$ at $z = 1 + H$ (where $H = d_g/d$). Given such a formal solution $T_g[T(z = 1)]$, we may then express the continuity of heat flux as

$$\partial_z T = \bar{\lambda}\, \partial_z T_g[T(z = 1)] \quad \text{at } z = 1 \tag{20}$$

where $\bar{\lambda} = \lambda_g/\lambda$ is the ratio of gas and liquid thermal conductivities.

We have now reached a generalized one-sided description of the problem, i.e. the system of equations (7-9) with boundary conditions (10, 11, 12, 20) is closed. However, such a problem is non-local, since the heat flux (20) depends on the instantaneous temperature *distribution* $T(z = 1)$ at the free surface (and not only on its local value).

Fortunately, this problem may easily be handled in Fourier space. Denoting the horizontal average by $\langle\cdot\rangle$, the horizontal Fourier transforms by tilded quantities, and realizing that from Eq. (19), $\langle T_g\rangle$ must vary linearly from $\langle T(z = 1)\rangle$ at $z = 1$ to T_{up} at $z = 1 + H$, the horizontal average of Eq. (20) yields

$$\partial_z \langle T\rangle = H^{-1}\bar{\lambda}\,(T_{up} - \langle T\rangle) \quad \text{at } z = 1 \tag{21}$$

which shows that the increase of heat transfer due to possible convection in the liquid is directly linked with the increase of the mean surface temperature.

Now, for Fourier components with wavenumber $k \neq 0$, Eq. (19) yields $(\partial_z^2 - k^2)\tilde{T}_g = 0$, which has to be solved with boundary conditions $\tilde{T}_g = \tilde{T}$

[4] Note that for this development to hold, it is necessary to assume that the gas phase is *confined*, i.e. its depth d_g must not be taken much larger than the liquid depth d. Moreover, the case of externally imposed fast gas flows is also excluded.

at $z = 1$ and $\tilde{T}_g = 0$ at $z = 1 + H$. Then, using this result in the Fourier transform of Eq. (20), we get

$$\partial_z \tilde{T} = -Bi_c(k)\tilde{T} \quad \text{at } z = 1 \tag{22}$$

where $Bi_c(k) = \bar{\lambda} k \coth(kH)$ is a generalized, *wavenumber-dependent* Biot number (i.e. dimensionless heat transfer coefficient, see end of §2.3). Nonlocality therefore manifests itself here through the fact that the different Fourier components of the temperature field evolve with different heat transfer coefficients at the upper free surface.

3.2 Generalized one-sided modeling of evaporation

When the liquid is volatile and evaporates into an inert gas such as air, the boundary condition (17) cannot be applied anymore, because the partial pressure of vapor cannot be assumed constant in general. Assuming the gas mixture to be perfect, we have $p_v = p_g N_g/(r + (1 - r)N_g)$ where p_g is the total gas pressure (assumed constant here, as can be justified *a posteriori*), $r = M/M_i$ is the ratio of molecular masses of the vapor and of the inert gas, and N_g is the vapor mass fraction for which a mass diffusion equation should be solved. The latter will here be written

$$\Delta N_g = 0 \tag{23}$$

i.e. in the quasi-steady approximation, just as for the temperature field in the previous section (these assumptions are coherent since the Lewis number $Le = D/\kappa$, where D is the isothermal diffusion coefficient, is of order unity for a gaseous mixture – hence the relaxation times in the gas are generally much smaller than those in the liquid, provided the depth of the gas is not too large).

In order to understand the basic role of an inert gas without entering into detailed descriptions of the gas phase dynamics, we will here consider that the mass fraction, just as the temperature, is imposed at the upper boundary, i.e.

$$N_g = N_{up} \quad \text{at } z = 1 + H \tag{24}$$

while at the interface, it will be assumed that the inert gas is not absorbed by the liquid, yielding

$$(1 - N_g)J + \bar{\rho}\bar{\kappa} Le \partial_z N_g = 0 \quad \text{at } z = 1 \tag{25}$$

where $\bar{\rho} = \rho_g/\rho$ and $\bar{\kappa} = \kappa_g/\kappa$ are the ratios of densities and of thermal diffusivities, respectively. Again, a Hertz-Knudsen kinetic equation is needed

for the evaporation rate J, which will here be written under the form

$$QJ = p_s(T_i) - \frac{N_i}{r + (1-r)N_i} \tag{26}$$

where $T_i = T(z=1)$ is the dimensionless interfacial temperature, $N_i = N_g(z=1)$ is the mass fraction of vapor at the interface, $p_s(T_i) = p_{eq}(T_i\theta)/p_g$ is the scaled saturation pressure, and the kinetic resistance to evaporation is quantified by

$$Q = \frac{\rho\kappa}{\beta d p_g}\sqrt{\frac{2\pi RT}{M}} \tag{27}$$

i.e. inversely proportional to the usual accomodation coefficient β.

Note that in the present treatment of evaporation, either for a pure vapor or for a gas mixture, possible motions of the interface are neglected, i.e. $z = h(t) \simeq 1$. This quasi-steady assumption is valid provided its relative motion during a typical relaxation time d^2/κ is small, i.e. $|\partial_t h| \ll 1$ in our choice of length and time scales. Actually, the total (jump) mass balance at the interface reads

$$J = W - \partial_t h = \bar{\rho}(W_g - \partial_t h) \quad \text{ at } z = h(t) \tag{28}$$

where W and W_g are vertical velocities of the liquid and of the gas mixture, respectively. Averaging in the horizontal direction and taking into account that $\langle W\rangle = 0$ because of Eqs (7) and (10), we get $\partial_t h = -\langle J\rangle$. Hence, the quasi-static approach will be valid provided the mean evaporation rate $\langle J\rangle$ is small enough compared to unity.

Another assumption is that the vertical velocity of the liquid at the interface is neglected, i.e. Eq. (11) is assumed, even though we should actually have $W(z=1) = J - \langle J\rangle$. This assumption, which may be checked a posteriori, should be valid provided typical velocities induced by the Marangoni (or Rayleigh) effect are much higher than the liquid velocity induced by evaporation[5].

In order to avoid nonlinearities in the mass transfer boundary conditions, and to remain coherent with the assumption of a small evaporation rate J, it

[5] In fact, in our choice of scales, $|J|$ is a typical Péclet number based on the liquid velocity induced by evaporation, and we assume it to be small in the present analysis. In turn, the Marangoni number $Ma = U_\gamma d/\kappa$ is another Péclet number based on the typical thermocapillary velocity $U_\gamma = \gamma\theta/\rho\nu$. As Ma is of order unity (or more), the ratio of thermocapillary and evaporation velocities is of order $Ma/|J| \gg 1$, which justifies Eq. (11), since the bulk value of W will always be much larger than $W(z=1)$. Note that the reasoning also holds for buoyancy-driven convection.

is convenient to assume the system to be close to a global equilibrium state defined by the overall gas pressure p_g (e.g., atmospheric) and the externally imposed vapor mass fraction N_{up}. At equilibrium, $J = 0$ and the mass fraction is equal to N_{up} everywhere in the gas, while both the liquid and the gas are at a temperature T^* determined by Eq. (26), i.e.

$$p_s(T^*) = \frac{N_{up}}{r + (1-r)N_{up}} \tag{29}$$

Then, assuming small deviations around this equilibrium state, boundary conditions (25) and (26) can be linearized, leading to

$$(1 - N_{up})J + \bar{\rho}\bar{\kappa}Le\partial_z N_g = 0 \quad \text{at } z = 1 \tag{30}$$

and

$$QJ = p_s'(T^*)(T_i - T^*) - \frac{r}{(r + (1-r)N_{up})^2}(N_i - N_{up}) \tag{31}$$

where Q is evaluated at the saturation temperature $T_{sat} = \theta T^*$.

Now, separating the horizontal average from the Fourier components with wavenumber k, as in section 3.1, we have to solve $\partial_z^2 \langle N_g \rangle = 0$ and $(\partial_z^2 - k^2)\tilde{N}_g = 0$ subject to corresponding boundary conditions. After some algebra, and taking into account that the complete interfacial energy balance reads $\partial_z T = \bar{\lambda}\partial_z T_g - EJ$ and that the thermal problem in the gas can be solved as before, we again get a mixed boundary condition

$$\partial_z \tilde{T} + Bi(k)\tilde{T} = 0 \quad \text{at } z = 1 \tag{32}$$

for the Fourier components with wavenumber $k \neq 0$, where the effective Biot number is now given by

$$Bi(k) = Bi_c(k) + Bi_{ev}(k) = \bar{\lambda}k\coth(kH) + \frac{Ep_s'(T^*)}{Q + \frac{H(1-N_{up})}{\bar{\rho}\bar{\kappa}Le}\frac{r(kH)^{-1}\tanh(kH)}{(r+(1-r)N_{up})^2}} \tag{33}$$

and the Fourier components of the evaporation rate are

$$\tilde{J} = E^{-1}Bi_{ev}(k)\tilde{T}_i = kH\coth(kH)\frac{\bar{\rho}\bar{\kappa}Le}{H(1-N_{up})}\tilde{N}_i \tag{34}$$

In addition, the horizontal average of the interfacial energy balance gives the boundary condition for $\langle T \rangle$, i.e.

$$\partial_z \langle T \rangle + Bi_{c,0}(\langle T \rangle - T_{up}) + Bi_{ev,0}(\langle T \rangle - T^*) = 0 \quad \text{at } z = 1 \tag{35}$$

where $Bi_{c,0} = Bi_c(k \to 0)$ and $Bi_{ev,0} = Bi_{ev}(k \to 0)$, while the averaged evaporation rate reads

$$\langle J \rangle = E^{-1} Bi_{ev,0}(\langle T_i \rangle - T^*) = \frac{\bar{\rho}\bar{\kappa} Le}{H(1 - N_{up})}(\langle N_i \rangle - N_{up}) \tag{36}$$

To summarize, this section has demonstrated that, in some vicinity of a global equilibrium state defined by the total gas pressure p_g and the vapor mass fraction N_{up} at some distance from the interface, convective evaporation of a pure liquid into an inert gas may be described by the system of equations (7-9), together with boundary conditions (10-12), (32) and (35). Note that additional reasonable assumptions are i) negligible gas viscosity; ii) sufficiently large gas thermal diffusivity; iii) not too large gas to liquid depth ratio H. This problem is not only nonlinear, but also non-local, as could be realized by applying an inverse Fourier transform to Eqs (32), leading to a convolution product. However, it is most convenient to write (and solve) it in Fourier space.

3.3 Reference states

Due to its symmetries, the full system of equations and boundary conditions always admits a horizontally homogeneous solution. On a long time scale, this solution evolves because of the decrease of the layer thickness in time. However, in the quasi-steady approximation described in the previous section, the free surface may be fixed at $z = 1$, and a steady solution exists, namely

$$\vec{V}_{ref} = 0 \ , \quad T_{ref} = T_{bot} - z \ , \quad p_{ref} = p_{bot} - Gaz + Ra\frac{z(1-z)}{2} \tag{37}$$

where the dimensionless temperature drop across the layer has been set to unity, by a suitable choice of the (yet undetermined) temperature scale

$$\theta = \frac{Bi_{c,0}(T_0 - T_H) + Bi_{ev,0}(T_0 - T_{sat})}{1 + Bi_{c,0} + Bi_{ev,0}} \tag{38}$$

as can be seen by solving Eq. (35) with $T_{bot} = T_0/\theta$, $T_{up} = T_H/\theta$ and $T^* = T_{sat}/\theta$. Note that T_{sat} depends on p_g and N_{up} according to our definition of the global equilibrium state. Now, using Eq. (36) and after some algebra, the evaporation rate in the non-equilibrium reference state (37) may be written as

$$J_{ref} = E^{-1}\frac{T_{i,c} - T^*}{Bi_{ev,0}^{-1} + (1 + Bi_{c,0})^{-1}} \tag{39}$$

where

$$T_{i,c} = \frac{T_{bot} + Bi_{c,0}T_{up}}{1 + Bi_{c,0}} = \frac{HT_{bot} + \bar{\lambda}T_{up}}{H + \bar{\lambda}} \tag{40}$$

is the interfacial temperature in a (fictive) purely conducting state, where evaporation is prevented (i.e. by assuming a vanishing accomodation coefficient leading to $Bi_{ev,0} = 0$).

It will be useful in the following to define

$$R_i = Q\ , \quad R_d = \frac{H(1-N_{up})}{\bar{\rho}\bar{\kappa}Le}\frac{r}{(r+(1-r)N_{up})^2}\ , \quad R_c = \frac{Ep'_s(T^*)H}{H+\bar{\lambda}} \tag{41}$$

and to recast Eq. (39) in the form

$$(R_i + R_d + R_c)J_{ref} = p'_s(T^*)(T_{i,c} - T^*) \tag{42}$$

which clearly shows (see also Haut and Colinet, 2005) that the evaporation flux is limited by three resistances "in series", namely the interfacial (kinetic) resistance R_i, the resistance R_d to diffusion in the gas mixture, and the resistance R_c to heat conduction towards the interface from both liquid and gas phases.

Other useful expressions for the reference evaporation rate can be found from Eqs (31), (36) and (42) :

$$(R_i + R_d)J_{ref} = p'_s(T^*)(T_{i,ref} - T^*) \tag{43}$$

$$(R_d + R_c)J_{ref} = p'_s(T^*)(T_{i,c} - T_{i,ref}) + \frac{r}{(r+(1-r)N_{up})^2}(N_{i,ref} - N_{up}) \tag{44}$$

$$(R_i + R_c)J_{ref} = p'_s(T^*)(T_{i,c} - T^*) - \frac{r}{(r+(1-r)N_{up})^2}(N_{i,ref} - N_{up}) \tag{45}$$

from which various limiting cases can be identified : i) when $R_c \ll R_d$ or $R_c \ll R_i$, comparing Eqs (42) and (43) readily shows that $T_{i,ref} = T_{i,c}$, i.e. the interfacial temperature is not affected by evaporation and reaches its value in the purely conducting state; ii) when $R_i \ll R_d$ or $R_i \ll R_c$, Eqs (42) and (44) lead to $p'_s(T^*)(T_{i,ref} - T^*) = r(N_{i,ref} - N_{up})/(r + (1 - r)N_{up})^2$, which means that local thermodynamic equilibrium prevails at the interface, according to Eq. (31); iii) when $R_d \ll R_c$ or $R_d \ll R_i$, Eqs (42) and (45) readily yield $N_{i,ref} = N_{up}$, and the gas composition is uniform. Clearly, two of these three situations may be realized simultaneously. For instance, in the case $R_i \gg R_d$ and $R_i \gg R_c$, the evaporation rate $J_{ref} = Q^{-1}p'_s(T^*)(T_{i,c} - T^*)$ is *reaction-limited*[6], even though this case should only

[6] Even though a phase transition is not a reaction, this term is used here to mean that the limitating step is linked to kinetic effects, i.e. the interface is not at equilibrium.